International Journal of
Intelligent Systems and Applications in Engineering

ISSN:2147-6799 www.ijisae.org Original Research Paper

Performance Evaluation of Different Feature Extractors and Classifiers for Recognition of Human Faces with Low Resolution Images

Soodeh Nikan*[1], Majid Ahmadi [2]

Accepted 15th August 2014 **DOI: 10.18201/ijisae.28949**

Abstract: Face recognition is an effective biometric identification technique used in many applications such as law enforcement, document validation and video surveillance. In this paper the effect of low resolution images which are captured in real world applications, on the performance of different feature extraction techniques combined with a variety of classification approaches is evaluated. Gabor features and its combination with local phase quantization histogram (GLPQH) are dimensionality reduced by principal component analysis (PCA), linear discriminant analysis (LDA), locally sensitive discriminant analysis (LSDA) and neighbourhood preserving embedding (NPE) to extract discriminant image characteristics and the class label is attributed using the extreme learning machine (ELM), sparse classifier (SC), fuzzy nearest neighbour (FNN) or regularized discriminant classifier (RDC). ORL and AR databases are utilized and the results show that ELM and RDC have better performance and stability against resolution reduction, especially on Gabor-PCA and Gabor-LDA techniques. Among the interpolation approaches that we employed to enhance the image resolution, nearest neighbour outperforms other methods.

Keywords: *Face recognition, Feature Extraction, Classification, Interpolation, Dimensionality Reduction.*

1. Introduction

Among the biometric identification technologies, face recognition is the most popular one due to its remarkable effectiveness and broad applications in video surveillance, law enforcement and human-computer interaction. The image degradations caused by illumination, pose and aging as well as variations in uncontrolled environment, affect the accuracy of face recognition algorithms significantly. Low-resolution images which are captured by video surveillance cameras, lead to noticeable decline in the identification performance. However, handling high resolution images and their storage is not cost effective and can increase the computational complexity of the recognition algorithm. In this paper, we examine the performance of different feature extraction techniques in combination with variety of classifiers with high and low resolution images. Furthermore, we evaluate the effect of image enhancement using various interpolation methods to improve the recognition accuracy. 2-D Gabor is a global feature descriptor where a Gaussian modulated by a sinusoid extracts the spatial frequency details of image [1]. Although it is a powerful descriptor to capture illumination invariant features, the high dimensionality of the feature vector burden computational complexity.

To reduce the size of feature vector, we use dimensionality reduction techniques, such as principal component analysis (PCA) [2], linear discriminant analysis (LDA) [3], locally sensitive discriminant analysis (LSDA) [4] and neighbourhood preserving embedding (NPE) [5]. We can also benefit from the local characteristic of local phase quantization (LPQ) [6] and combine it with Gabor filter to reduce the effect of blur variation. In the classification stage we examine the performance of four different classifiers. Regularized discriminant classifier (RDC) [7], fuzzy nearest neighbour (FNN) [8], sparse classifier (SC) [9] and extreme learning machine (ELM) [10] are utilized in this paper. Low resolution images are enhanced using the interpolation techniques such as nearest neighbour, bilinear and bicubic interpolation [11].

The rest of paper is as follows. In section.2 and 3, feature extraction approaches are explained. Different classifier techniques are explained in section.4. Section.5 is related to the interpolation methods to enhance the image resolution. Section.6, shows the experimental results and comparisons. The paper is concluded in section.7.

2. Feature Extraction

2.1. Gabor

Representation of 2-D Gabor resembles the human visual system and a set of Gabor filters can extract image characteristics in different orientations and frequencies which are robust against appearance variations. Gabor filter is a Gaussian kernel multiplied by a sinusoid function as follows [1, 12].

$$\psi_{s,o}(x,y) = \frac{{f_s}^2}{\pi\gamma\mu} \cdot e^{-\left[\left(\frac{{f_s}^2\hat{x}^2}{\gamma^2}\right)+\left(\frac{{f_s}^2\hat{y}^2}{\mu^2}\right)\right]} \cdot e^{-(j2\pi.f_s.\hat{x})} \quad (1)$$

Where,

$$\begin{cases} s = 0, 1, 2, \dots, S_{max} - 1 \\ o = 0, 1, 2, \dots, O_{max} - 1 \\ \hat{x} = +x\cos(\beta_o) + y\sin(\beta_o) \\ \hat{y} = -x\sin(\beta_o) + y\cos(\beta_o) \end{cases} \quad (2)$$

[1] *ECE, University of Windsor, Windsor, ON – N9B 3P4, Canada*
[2] *ECE, University of Windsor, Windsor, ON – N9B 3P4, Canada*
** Corresponding Author: Email: nikan@uwindsor.ca*
Note: *This paper has been presented at the International Conference on Advanced Technology&Sciences (ICAT'14) held in Antalya (Turkey), August 12-15, 2014.*

$\beta_o = (o\pi)/8$, $f_s = f_{max}/(\sqrt{2})^s$ where, f_{max} is the maximum frequency of the filter. S_{max} and O_{max} are the maximum number of scale and orientation, respectively. γ and μ, both equal to $\sqrt{2}$, are the sharpness of x and y axis, respectively. Therefore, we have a set of $S_{max} \times O_{max}$ filters which are convolved with the image to obtain the Gabor images. All Gabor coefficients are combined as a high dimension feature vector. To reduce the size of feature vector and computation cost, a dimensionality reduction approach is applied such as PCA, LDA, LSDA and NPE [12, 13].

2.2. GLPQH

Combination of Gabor filter with LPQ leads to distinctive local image characteristics which are blur invariant. LPQ, which is applied on the Gabor images, is a well-known histogram-based and blur invariant feature extractor that performs the local phase analysis at four frequency components in a small neighborhood around each image pixel [6]. The point spread function (PSF) of blur effect is centrally symmetric and its phase is zero at small frequencies within the bandwidth of PSF and thus the phase analysis is blur invariant. Therefore, assessment and binary quantization of the real and imaginary parts of the frequency components of short term Fourier transform (STFT) components at those frequencies, gives an 8-bit pattern for each pixel of image [6] as shown in (Figure.1). Thus, we have a histogram of 256 bins for each Gabor image, concatenation of which leads to a feature vector of size $S_{max} \times O_{max} \times 256$. Dimensionality reduction techniques in section 3 are employed to reduce the size of feature vector. The whole procedure is shown in (Figure.2).

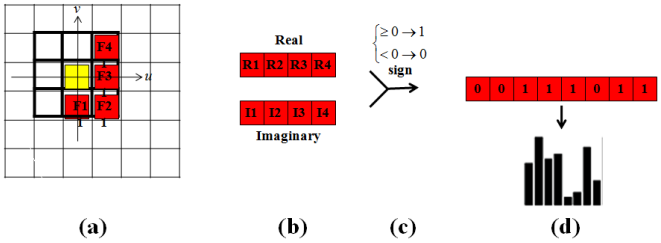

Figure 1. LPQ procedure: (a) STFT at four specific frequencies inside a small window at the pixel position, (b) finding the real and imaginary of the four STFT values, (c) binary quantization based on the sign of real and imaginary values, and (d) constructing a histogram based on the 8-bit bit stream

3. Dimensionality Reduction Techniques

3.1. Principal Component Analysis (PCA)

PCA is an unsupervised linear dimensionality reduction approach. This holistic-based technique utilize the whole face image and transforms the image pixels to eigenspace which is a lower dimension subspace [2]. The mean image is calculated by averaging the gallery set. After subtracting the mean image from the gallery samples, the covariance matrix is calculated as follows [12, 2].

$$Cov = \frac{1}{N_I}\sum_{k=1}^{N_I}(I_k - M).(I_k - M)^T \quad (3)$$

Where, I_k is the k^{th}gallery sample, N_I is the number of gallery images and M is the mean image. The eigenvalues are sorted in descent order. The eigenvectors of the covariance matrix corresponding to a few number of largest eigenvalues are utilized to transform the gallery and probe images to eigenspace, which are called eigenfaces [12, 2].

$$\lambda.V = Cov.V \quad , \quad \widehat{I_i} = V^T.(I_i - M) \quad (4)$$

Where, λ and V are the eigenvalue and eigenvector, respectively. I_i is the i^{th} image sample and $\widehat{I_i}$ is its corresponding eigenface [12].

3.2. Linear Discriminant Analysis (LDA)

LDA reduces dimension linearly by maximizing the ratio of between-class to the within-class scatter matrix as follows [3].

$$S_b = \sum_{k=1}^{N_c} N_{c_k}.(M_k - M).(M_k - M)^T \quad (5)$$

$$S_w = \sum_{k=1}^{N_c}\sum_{I_i \epsilon C_i}(I_i - M_k).(I_i - M_k)^T \quad (6)$$

$$V_{opt} = argmax(\frac{V^T.S_b.V}{V^T.S_w.V}) \quad (7)$$

Where, N_c and $N_{c_k}$are the number of classes and samples in the k^{th} class, respectively. C_i is i^{th} subject, M_k and M are the mean of gallery samples and samples in k^{th} class, and S_w and S_b are the within and between-class scatter matrices respectively. $S_b.V = \lambda.S_w.V$ gives the eigenvector, V, [12, 3].

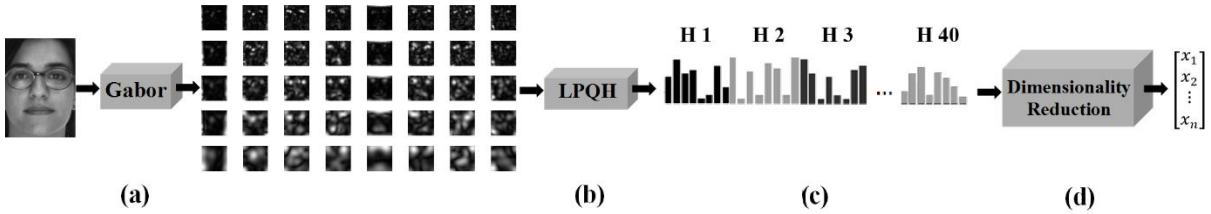

Figure 2. Proposed GLPQH technique to extract feature vector of image: (a) Gabor filtering of the image, (b) applying LPQ on each filtered image and find the histograms, (c) concatenate the histograms, and (d) dimensionality reduction PCA, LDA, LSDA or NPE

3.3. Locally Sensitive Discriminant Analysis (LSDA)

LSDA is a linear data analysis technique to reduce the data

dimension, with small number of gallery samples, based on the local geometrical structure of data according to the adjacency graph where the data points are nodes and there are edges with weight equal to one between each node and its k nearest neighbours [4]. Due to the fact that in this method, the emphasis is on data discrimination, the graph of neighbours with the same class label is separated from the between class adjacent subset [4]. The aim is to find a data projection solution to map the adjacent graphs in such a way so that within-class nodes be as close as possible and between-class nodes stay as far as possible. Thus, the following maximum eigenvalue problem is required to be solved and the projection matrix is constructed of the eigenvectors, v, corresponding to m highest eigenvalues, λ, which are sorted in order [4].

$$S(\alpha\Phi_b + (1-\alpha W_w))S^T v = \lambda S D_w S^T v \quad (8)$$

Where, $S = (s_1, s_2, \dots, s_N)$ is the set of sample points, W_w and D_w are the within-class graph weight matrix and its column-sum, respectively. $\Phi_b = W_b - D_b$, where, W_b and D_b are the between-class graph weight matrix and its column-sum, respectively, and $V_{N\times m}$ is the projection matrix (mathematical details can be found in [4]).

3.4. Neighbourhood Preserving Embedding (NPE)

NPE is a linear dimensionality reduction method where we first construct the adjacency graphs with N sample points as the nodes. There would be edges from each node to its k nearest neighbours. The weights on adjacent edges are calculated by minimization of the objective function as follows [5].

$$\psi(w) = min \sum_i \left\| s_i - \sum_j w_{ij} s_j \right\|^2 \quad (9)$$

Then we need to find the projection matrix by calculating the eigenvalues λ, and eigenvectors v.

$$SLS^T v = \lambda S S^T v \quad (10)$$

Where, $S = (s_1, s_2, \dots, s_N)$ is the set of sample points, $L = (I-w)^T(I-w)$ and I is the Identity matrix. Thus, the projected sample is calculated using the projection matrix V of size$N \times m$, which is composed of the eigenvectors corresponding to m largest eigenvalues [5].

$$\widehat{s_i} = V^T . s_i , \quad where \quad V = (v_1, v_2, \dots, v_m) \quad (11)$$

4. Classification techniques

4.1. Regularized Discriminant Classification (RDC)

Discriminant analysis classification is based on the normal distribution as follows [7].

$$G_i(\bar{F}) = (2\pi)^{-\frac{N}{2}} \left|\delta_i\right|^{-\frac{1}{2}} e^{-\frac{1}{2}(\bar{F}-\mu_i)^T \delta_i^{-1} (\bar{F}-\mu_i)} \quad (12)$$

Where, μ_k and δ_k are the mean and covariance of the samples in class $i, (0 < i < C)$, and C is the number of individuals, respectively. $\bar{F} = (f_1, f_2, \dots, f_N)$ is the feature vector of a sample with N features. The quadratic discriminant function (the special case of which is linear discriminant) is as follows [7].

$$D_i(\bar{F}) = (\bar{F} - \mu_i)^T . \delta_i^{-1} . (\bar{F} - \mu_i) + ln|\delta_i| - 2ln\pi_i \quad (13)$$

Where, $2ln\pi_i$ is the Mahalanobis distance between $\bar{F}$ and μ_i. RDC is the regularized form of discriminant classification by adding regularization values to class scatter matrix [7].

$$D^R{}_i(\bar{F}) = (\bar{F} - \mu_i)^T . \delta_i^{-1}(\rho,\gamma) . (\bar{F} - \mu_i) + ln|\delta_i(\rho,\gamma)| - 2ln\pi_i \quad (14)$$

Where, ρ, γ are the regularization parameters ($\rho, \gamma \in [0,1]$) [7].

4.2. Fuzzy Nearest-Neighbour (FNN)

In the nearest neighbour classifier we assign a class to a probe sample which has the minimum distance to the gallery sample of the corresponding class and do not take the contribution of each labelled sample in attributing the class label which leads to misclassification when samples overlap [8]. However, in fuzzy nearest neighbour classification the fuzzy membership values per class are devoted to the sample and decision is made according to the maximum vote which increases the classification confidence. The class membership is calculated using the Euclidean distance between the sample and the class means prototype as follows [8].

$$w_i(s) = \frac{\|s - M_i\|^{-\frac{2}{m-1}}}{\sum_{j=1}^{C} \|s - M_j\|^{-\frac{2}{m-1}}} \quad (15)$$

Where, $w_i(s)$ is the membership value of sample s in the i^{th} class, M_i is the mean of i^{th} class and C is the number of classes.

4.3. Sparse Classifier(SC)

Sparse classifier which is based on the sparse representation is the general form of nearest neighbour technique and has a remarkable discriminative power [9]. The probe samples can be represented sparsely as a linear combination of gallery samples of the same individual .The sparsest representation can be achieved by using the l_1-norm [13, 9]. The matrix of gallery samples is as follows.

$$G = [G_1, G_2, G_3, \dots, G_N] \quad (16)$$

$$G_i = \left[F_1^g, F_2^g, F_3^g, \dots, F_L^g\right] \quad (17)$$

Where, G_i is the matrix of gallery images of the i^{th} class and F_k^g is the feature vector of the k^{th} sample in G_i. N and L are the number of individuals and gallery samples per class, respectively. A probe sample is represented as follows [13].

$$F_i^p = G.C \quad (18)$$

Where, $C = [0,0,\dots,0, c_1^i, c_2^i, \dots, c_L^i, 0,0,\dots,0]$ and c_j^i is the j^{th} coefficient associated with the i^{th}class.

In order to find the identity of the probe sample, we require to solve the l_1-norm minimization problem as follows [13].

$$(l_1): \quad \hat{C}_1 = argmin\|C\|_1 \quad while \ F^p = G.C \tag{19}$$

4.4. Extreme Learning Machine (ELM)

Feed forward neural networks are slow in learning and poor in scalability since they have to tune the weights iteratively via the gradient descent approach which is very slow. Extreme learning machine is a generalized form of single hidden layer neural networks with random hidden nodes where the weights of hidden layer are determined and do not require to be adjusted in iterations [13, 10]. Therefore, it is significantly faster than feed forward neural networks which is an important issue in pattern recognition problems.

5. Interpolation

In real word applications, the captured images usually have very low resolution which degrades the accuracy of the identification algorithm. In order to enhance the image resolution, one of the image interpolation techniques is required to enlarge the probe image. In this paper we have employed the nearest neighbour, bilinear and bicubic interpolation methods to increase the image resolution before applying the face recognition algorithm on the image.

5.1. Nearest Neighbour Interpolation

This method is the fastest and simplest interpolation technique based on copying the grey value of the nearest neighbour of the reference pixel which leads to a larger image [11].

5.2. Bilinear Interpolation

In bilinear technique the intensity value of each unknown pixel is predicted using a weighted combination of the grey values of four neighbours. The resulting image is smoother than the nearest neighbour interpolated image [11].

5.3. Bicubic Interpolation

In order to find the intensity value of the interpolated pixels, we calculate the convolution of a cubic function with the 4×4 neighbourhood around the reference pixel [11].

6. Experimental Results

6.1. Databases and Simulation Settings

In order to evaluate the performance of the proposed feature extraction and classification combinations, we utilize ORL and AR databases. Gabor filter has 8 scales, 5 orientations and f_max=0.25. The value of m in FNN is equal to 2 and 0.1 is selected as the regularization factor in RDC, which are chosen experimentally through an exhaustive search.

ORL: AT&T or Olivetti research lab (ORL) database which consists of 400 images of 40 people (10 per individual) of size 112×92 with different time, scales and illumination conditions, and various facial expressions (open/close eyes and smiling/not smiling) and up to 20 degree tilting and rotation [14]. We use the first 5 samples of each individual in the gallery and the rest 5 images in the probe dataset. Therefore, we have 200 images in the gallery set and 200 in the probe set.

AR: AR face database contains more than 3000 facial images of 136 people (76 men and 60 women) [15]. 26 images of each individual were taken in two sessions in two weeks (13 images per session). The database consists of eye aligned images of size 165×120 pixels with illumination variation, facial expression and partial occlusion [15]. We have employed non-occluded images 1 to 4 with different facial expressions in session 1 as the gallery and non-occluded images 2 to 4 in session 2, with appearance changes in time gap and facial expression and illumination variation, as the probe set.

6.2. Experiment I

In the first experiment we employed the proposed feature extraction and classification algorithms on the images of size 128×128 pixels in the mentioned datasets and the results are shown in (Table.1 & 2) for ORL and AR databases, respectively.

Table 1. Identification accuracies (%) for 128×128 pixels images in ORL database with different combinations of feature extraction and classification techniques

Classification Feature Extraction	FNN	ELM	SC	RDC
Gabor-PCA	96	99.5	97.5	99
Gabor-LDA	98	99.5	98	99
Gabor-LSDA	96.5	99.5	97.5	96.5
Gabor-NPE	99	96.5	96.5	98
GLPQH- PCA	93	95	96.5	95
GLPQH- LDA	94.5	93.5	95	94.5
GLPQH- LSDA	92.5	90.5	91	93
GLPQH- NPE	88	91.5	92	89

We repeat the experiment for low resolution images of size 16×16 pixels and (Table.3 & 4) illustrate the results for ORL and AR databases, respectively.

Table 2. Identification accuracies (%) for 128×128 pixels images in AR database with different combinations of feature extraction and classification techniques

Classification Feature Extraction	FNN	ELM	SC	RDC
Gabor-PCA	83	96.33	92.33	93.67
Gabor-LDA	96.33	96.33	95.67	96.67
Gabor-LSDA	74.67	96.33	86	75.67
Gabor-NPE	78	96.33	89	79
GLPQH- PCA	89.33	87.67	93	92
GLPQH- LDA	93	90	92	92.33
GLPQH- LSDA	48.67	81.33	55.67	47.33
GLPQH- NPE	45.33	87	55	44.33

The results show that utilizing PCA and LDA as dimensionality reduction techniques leads to better results for both databases. ELM has the best average performance for both databases. FNN shows the least stability versus resolution reduction for all feature extraction methods.

Table 3. Identification accuracies (%) for 16 × 16 pixels images in ORL database with different combinations of feature extraction and classification techniques

Classification Feature Extraction	FNN	ELM	SC	RDC
Gabor-PCA	94	95.5	97	97
Gabor-LDA	95.5	95.5	93.5	96
Gabor-LSDA	94	95.5	94.5	95.5
Gabor-NPE	90.5	94	94	94
GLPQH- PCA	96.5	97	95.5	96
GLPQH- LDA	96.5	97	95.5	96
GLPQH- LSDA	96.5	96	95	96.5
GLPQH- NPE	96.5	97.5	96.5	93.5

Table 4. Identification accuracies (%) for 16 × 16 pixels images in AR database with different combinations of feature extraction and classification techniques

Classification Feature Extraction	FNN	ELM	SC	RDC
Gabor-PCA	64.33	79.33	72.33	72.67
Gabor-LDA	68	67.33	68.67	70.33
Gabor-LSDA	49.67	67	51	50.33
Gabor-NPE	52.67	67.68	51.67	52.33
GLPQH- PCA	59.33	67.67	65.33	69.33
GLPQH- LDA	71.67	69.33	70.33	67.33
GLPQH- LSDA	54.33	69	61	54.33
GLPQH- NPE	57.33	68.33	61.33	56.67

6.3. Experiment II

In this experiment we apply three interpolation techniques on 16×16 images to enhance the resolution to the size of 128×128 and then apply the face recognition techniques. (Figure.3 & 4) illustrate the results on ORL and AR databases, respectively.
Nearest neighbour interpolation performs better than the other two methods for the ORL database and with Gabor technique the results are very close to the recognition rates in (Table.1).
(Figure.4) shows that the bicubic and bilinear methods performances are comparable, but nearest neighbour interpolation outperforms those two approaches and ELM shows almost consistent performance in combination with all feature extraction techniques.

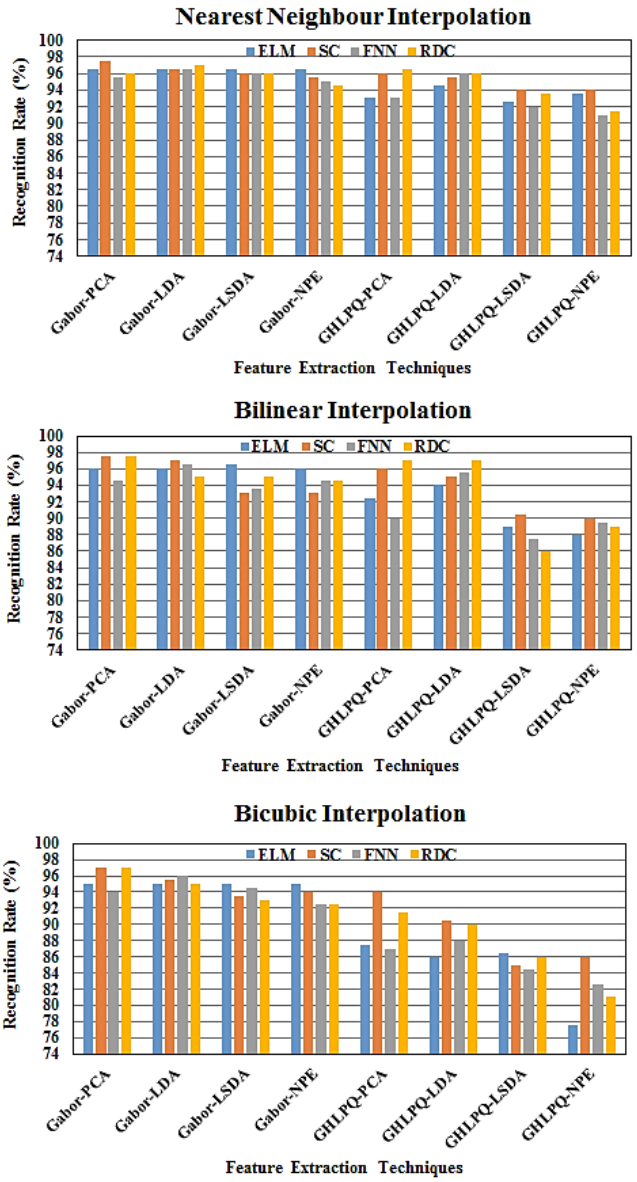

Figure 3. Recognition accuracies (%) for different feature extraction and classification combinations on the interpolated images in ORL database (from 16 × 16 pixels to 128 × 128 pixels) with three interpolation techniques; nearest neighbour, bilinear and bicubic

7. Conclusion

In this paper we have evaluated the performance of face recognition algorithms on low resolution images of the ORL and AR databases and the effect of interpolation techniques to enhance their results. We have used different combinations of feature extraction and classification approaches. Gabor and its combination with LPQ histogram (GLPQH) are utilized as image descriptors and to deal with the high dimensionality problem we have used PCA, LDA, LSDA and NPE methods. Extreme learning machine, sparse classifier, fuzzy nearest neighbour and regularized discriminant classifiers are employed to assign the class labels. The results of experiments show that ELM and RDC have acceptable performance and stability against resolution reduction, especially in combination with Gabor technique with LDA or PCA dimensionality reduction. Nearest neighbour interpolation outperforms bilinear and bicubic interpolations in order to enhance the low resolution image.

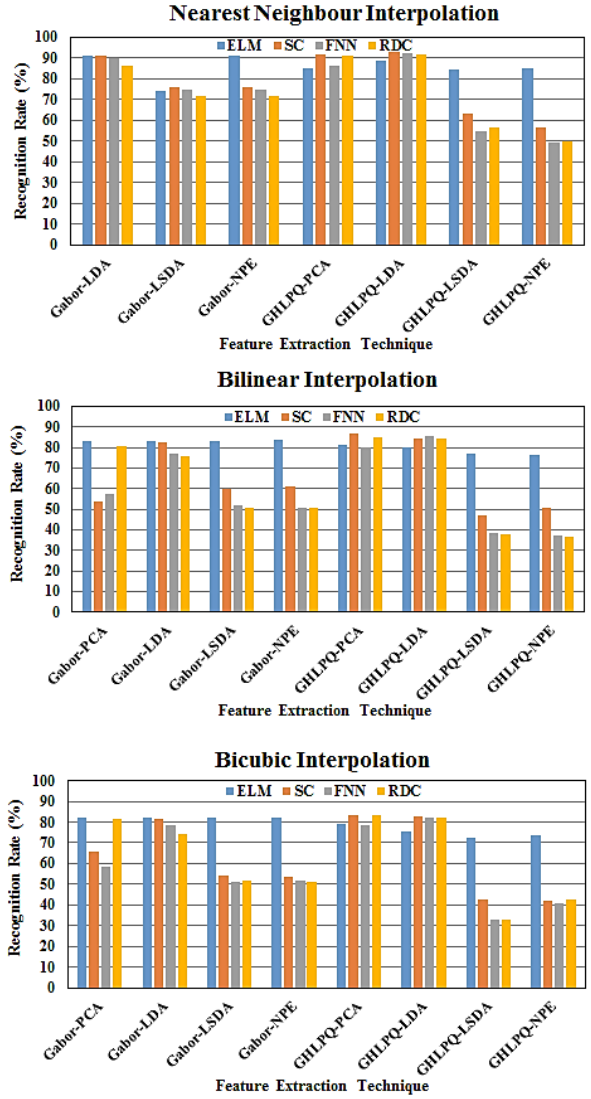

Figure 4. Recognition accuracies (%) for different feature extraction and classification combinations on the interpolated images in AR database (from 16 × 16 pixels to 128 × 128 pixels) with three interpolation techniques; nearest neighbour, bilinear and bicubic

References

[1] J. Daugman (1998). Complete Discrete 2-D Gabor Transform by Neural Networks for Image Analysis and Compression. IEEE Transaction on Acoustic, Speech and Signal Processing. Vol.36. Pages.1169-1179.

[2] M. Turk and A. Pentland (1991). Eigenfaces for Recognition. Journal of Cognitive Neuroscience. Vol.3. Pages.71-86.

[3] K. Etemad and R. Chellappa (1997). Discriminant Analysis for Recognition of Human Face Images. Journal of Optical Society of America A. Vol.14. Pages.1724-1733.

[4] D. Cai, X. He, K. Zhou, J. Han and H. Bao (2007). Locality Sensitive Discriminant Analysis. Proc. IJCAI'07. Pages. 708-713.

[5] X. He, D. Cai, S. Yan and H. J. Zhang (2005). Neighborhood Preserving Embedding. Proc. ICCV'05. Pages.1208-1213.

[6] C. H. Chan, M. A. Tahir, J. Kittler and M. Pietikainen (2013). Multiscale Local Phase Quantization for Robust Component-Based Face Recognition Using Kernel Fusion of Multiple Descriptors. IEEE Transactions on Pattern Analysis and Machine Intelligence. Vol.35. Pages.1164-1177.

[7] J. H. Friedman (1989). Regularized Discriminant Analysis. Journal of the American Statistical Association. Vol.84. Pages.165-175.

[8] J. M. Keller, M. R. Gray and J. A. Givens (1985). A Fuzzy K-Nearest Neighbor Algorithm. IEEE Transactions on Systems, Man and Cybernetics. Vol.15. Pages.580-585.

[9] J. Wright, A.Y. Yang, A. Ganesh, S. S. Sastry and Y. Ma (2009). Robust Face Recognition via Sparse Representation. IEEE Transactions on Pattern Analysis and Machine Intelligence. Vol.31. Pages.210-227.

[10] G. B. Huang, H. Zhou, X. Ding and R. Zhang (2012). Extreme Learning Machine for Regression and Multiclass Classification. IEEE Transactions on Systems, Man and Cybernetics. Vol.45. Pages.513-529.

[11] S. M. Metev and V. P. Veiko (2011). Practical Image And Video Processing Using MATLAB. New Jersey: John Wiley & Sons. Hoboken 1st ed.

[12] S. Nikan and M. Ahmadi (2014). Study of The Effectiveness of Various Feature Extractors for Human Face Recognition for Low Resolution Images. Proc. AISE'05. Pages. 1-6.

[13] S. Nikan and M. Ahmadi (2014). Effectiveness of Various Classification Techniques on Human Face Recognition. Proc. HPCS'14. In Press.

[14] The AT&T Laboratories Cambridge Website. [Online]. Available:

[15] http://www.cl.cam.ac.uk/research/dtg/attarchive/facedatabase.html.

[16] A. Martinez and R. Benavente (1998). The AR Face Database. CVC Technical Report. Vol. 24. [Online]. Available:

[17] <http://www2.ece.ohio-state.edu/~aliex/ARdatabase.html>.